

Integrated Design of Speed Sensorless Control Algorithms for Induction Motors

Zhang, J.; Wang, Y.; Bortoff, S.A.; Satake, A.; Furutani, S.; Deng, X.

TR2015-093 July 30, 2015

Abstract

Bandwidth limitation hinders the economical and broad application of induction motors promised by speed sensorless drive. This paper proposes an integrated control and observer design for speed sensorless control of induction motors with stator voltage and current measurements. With a general observer structure, the backstepping-based robust control design explicitly considers the errors of both the state estimation and tracking, and thus avoids the commonly used time scale separation. The gain selection for the controller becomes easy and straightforward. As a case study, the extended Kalman filter is used as a state estimator in order to simplify the gain tuning process. Simulation results validate the effectiveness of proposed method.

2015 Chinese Control Conference (CCC) & SICE Annual Conference

This work may not be copied or reproduced in whole or in part for any commercial purpose. Permission to copy in whole or in part without payment of fee is granted for nonprofit educational and research purposes provided that all such whole or partial copies include the following: a notice that such copying is by permission of Mitsubishi Electric Research Laboratories, Inc.; an acknowledgment of the authors and individual contributions to the work; and all applicable portions of the copyright notice. Copying, reproduction, or republishing for any other purpose shall require a license with payment of fee to Mitsubishi Electric Research Laboratories, Inc. All rights reserved.

Integrated Design of Speed Sensorless Control Algorithms for Induction Motors

Jian Zhang¹, Yebin Wang², Scott A. Bortoff², Akira Satake³, Shinichi Furutani³, Xinyan Deng¹, Bin Yao¹

1. School of Mechanical Engineering, Purdue University, 585 Purdue Mall, West Lafayette, IN 47907 USA.

E-mail: zhang699@purdue.edu, xdeng@purdue.edu

2. Mitsubishi Electric Research Laboratories, 201 Broadway, Cambridge, MA 02139 USA.

E-mail: yebinwang@ieee.org, bortoff@merl.com

3. the Advanced Technology R&D Center, Mitsubishi Electric Corporation, 8-1-1, Tsukaguchi-honmachi, Amagasaki City, 661-8661, Japan.

E-mail: Satake.Akira@dy.MitsubishiElectric.co.jp, Furutani.Shinichi@dw.MitsubishiElectric.co.jp

Abstract: Bandwidth limitation hinders the economical and broad application of induction motors promised by speed sensorless drive. This paper proposes an integrated control and observer design for speed sensorless control of induction motors with stator voltage and current measurements. With a general observer structure, the backstepping-based robust control design explicitly considers the errors of both the state estimation and tracking, and thus avoids the commonly used time scale separation. The gain selection for the controller becomes easy and straightforward. As a case study, the extended Kalman filter is used as a state estimator in order to simplify the gain tuning process. Simulation results validate the effectiveness of proposed method.

Key Words: Speed sensorless control, induction motor, extended Kalman filter, backstepping

1 Introduction

Speed regulation of induction motors is an old but interesting problem. Techniques to achieve the speed regulation have evolved from variable frequency control to vector control and its variants for instance direct/indirect field-oriented state feedback control, speed-sensorless control [1, 2], adaptive field-oriented control [1, 3]. The vector control with full state or the rotor speed measurements results in good performance at expenses of extra sensors, and thus limits its application in practice. Recent work is devoted to speed sensorless control algorithms, e.g. without the speed measurement.

Speed-sensorless control design problem is practically meaningful and challenging, and thus attracts a lot of theoretical interests, e.g. [4, 5]. Adaptive idea, where the rotor speed is typically treated as an unknown parameter to avoid nonlinearity in dynamics, was initially exploited and is still prevailing in the speed-sensorless motor drives [6–10]. Designs relying on the assumption of the speed as a constant/slow-varying parameter suffer unsatisfactory transient performance inherent to adaptation. Numerous work tried to avoid the speed-as-parameter assumption for instance high gain observer [2], sliding mode observer [11–13], and extended kalman filter (EKF) [14] etc., but failed to address the drive performance aspect. As an example, resorting to nonlinear observer design techniques entails the system in certain normal forms, which turns out to be difficult. Well-known high gain observer design assumes observable form (OF). The induction motor model under any frame is hardly put into OF due to the complexity of the state transformation and difficulty to compute the inverse transformation. Various work circumvented the problem by considering open-loop flux observer, e.g. [2], thus lead to drives with slow responses.

This paper proposes an integrated control and observer design framework for speed sensorless control of induction

motors with stator current measurements. With a general observer structure, the backstepping-based robust control design explicitly considers all the state estimation and tracking errors. The gain selection for the controller is straightforward. On the state estimation side, as a case study, an extended Kalman filter is designed to simplify the gain tuning process. Simulation results are presented to show the following facts: 1) the proposed method can achieve high bandwidth and high precision speed sensorless tracking control of a typical induction motor under practical constraints (200Hz control bandwidth for 20KHz sampling rate); 2) the gain selection for the proposed method is systematic and simple; 3) the proposed method can track various trajectories as long as the state and control input constraints are considered. No dependence of controller and/or observer on the trajectory is found.

2 Preliminaries

2.1 The Induction Motor Model

With the assumption of linear magnetic circuits and balanced operating conditions, the two-phase equivalent model of an induction motor, represented in the fixed a - b reference frame, can be written as follows [15],

$$\begin{aligned}\dot{\omega} &= \frac{3n_p M}{2JL_r}(\phi_{ra}i_{sb} - \phi_{rb}i_{sa}) - T_L/J, \\ \dot{i}_{sa} &= \frac{MR_r}{\sigma L_r^2}\phi_{ra} + \frac{n_p M}{\sigma L_r}\omega\phi_{rb} - \gamma i_{sa} + \frac{1}{\sigma}u_{sa}, \\ \dot{i}_{sb} &= \frac{MR_r}{\sigma L_r^2}\phi_{rb} - \frac{n_p M}{\sigma L_r}\omega\phi_{ra} - \gamma i_{sb} + \frac{1}{\sigma}u_{sb}, \\ \dot{\phi}_{ra} &= -\frac{R_r}{L_r}\phi_{ra} - n_p\omega\phi_{rb} + \frac{R_r}{L_r}Mi_{sa}, \\ \dot{\phi}_{rb} &= -\frac{R_r}{L_r}\phi_{rb} + n_p\omega\phi_{ra} + \frac{R_r}{L_r}Mi_{sb}, \\ y &= [i_{sa}, i_{sb}]^T,\end{aligned}\quad (1)$$

where the subscripts r and s stand for the stator and the rotor, respectively; the subscripts a and b denote the a and b axis,

This work was done while J. Zhang was an intern with Mitsubishi Electric Research Laboratories, 201 Broadway, Cambridge, MA 02139 USA.

respectively; ω is the angular speed of the rotor, i denotes the current, and ϕ denotes the flux linkage; u is the stator voltage input; R, L, M, J, T_L and n_p denote the resistance, inductance, mutual inductance, rotor inertia, load torque, and number of pole pairs, respectively. For compact notations, following lumped parameters are introduced with $\alpha = \frac{R_r}{L_r}$, $\beta = \frac{M}{\sigma L_r}$, $\sigma = L_s - \frac{M^2}{L_r}$, $\gamma = \frac{M^2 R_r + L_r^2 R_s}{\sigma L_r^2} = \frac{R_s}{\sigma} + \alpha\beta M$, and $\mu = \frac{3}{2} \frac{n_p M}{J L_r}$. We assume that the load torque T_L can be parameterized as $T_L(\omega) = T_0 + C_f \omega$ with T_0 an unknown constant. With the following change of notations, $x_1 = \omega$, $x_2 = i_{sa}$, $x_3 = i_{sb}$, $x_4 = \phi_{ra}$, $x_5 = \phi_{rb}$, $u_1 = u_{sa}$, $u_2 = u_{sb}$, $b = \frac{1}{\sigma}$, $a_1 = \mu$, $a_2 = \frac{T_0}{J}$, $a_3 = \frac{C_f}{J}$, $a_5 = \alpha\beta$, $a_6 = n_p\beta$, $a_7 = \gamma$, $a_8 = \alpha$, $a_9 = n_p$, and $a_{10} = \alpha M$, one can rewrite the induction model (1) as

$$\begin{aligned} \dot{x} &= f(x, u) = g(x) + Bu, \\ y &= Cx, \\ g(x) &= \begin{bmatrix} a_1(x_3x_4 - x_2x_5) - a_2 - a_3x_1 \\ a_5x_4 + a_6x_1x_5 - a_7x_2 \\ a_5x_5 - a_6x_1x_4 - a_7x_3 \\ -a_8x_4 - a_9x_1x_5 + a_{10}x_2 \\ -a_8x_5 + a_9x_1x_4 + a_{10}x_3 \end{bmatrix}, \\ B &= \begin{bmatrix} 0 & 0 \\ b & 0 \\ 0 & b \\ 0 & 0 \\ 0 & 0 \end{bmatrix}, \quad C = \begin{bmatrix} 0 & 1 & 0 & 0 & 0 \\ 0 & 0 & 1 & 0 & 0 \end{bmatrix}, \end{aligned} \quad (2)$$

with $x = [x_1, x_2, x_3, x_4, x_5]^T$ and $u = [u_1, u_2]^T$.

2.2 Problem Formulation

General specifications for speed-sensorless electric drives using vector control is to regulate two variables: the rotor speed and the rotor flux magnitude [1, 2] given by

$$\begin{bmatrix} x_1 \\ x_4^2 + x_5^2 \end{bmatrix}. \quad (3)$$

More specifically, the problem considered in this work is: Given the IM model (2), synthesize control inputs u_1 and u_2 such that x_1 and $x_4^2 + x_5^2$ track $\omega_d(t)$ and ψ_d^2 , respectively.

3 Main Results: Observer Design

3.1 A General Observer

For the integrated design of observer and controller, a general observer structure is first assumed as $\hat{x}_i = \dot{f}_i + si_i, 1 \leq i \leq 5$, i.e.,

$$\begin{aligned} \dot{\hat{x}}_1 &= a_1(x_3\hat{x}_4 - x_2\hat{x}_5) - \hat{a}_2 - a_3\hat{x}_1 + si_1(\tilde{x}_2, \tilde{x}_3) \\ \dot{\hat{x}}_2 &= a_5\hat{x}_4 + a_6\hat{x}_1\hat{x}_5 - a_7\hat{x}_2 + bu_1 + si_2(\tilde{x}_2, \tilde{x}_3) \\ \dot{\hat{x}}_3 &= a_5\hat{x}_5 - a_6\hat{x}_1\hat{x}_4 - a_7\hat{x}_3 + bu_2 + si_3(\tilde{x}_2, \tilde{x}_3) \\ \dot{\hat{x}}_4 &= -a_8\hat{x}_4 - a_9\hat{x}_1\hat{x}_5 + a_{10}\hat{x}_2 + si_4(\tilde{x}_2, \tilde{x}_3) \\ \dot{\hat{x}}_5 &= -a_8\hat{x}_5 + a_9\hat{x}_1\hat{x}_4 + a_{10}\hat{x}_3 + si_5(\tilde{x}_2, \tilde{x}_3) \end{aligned} \quad (4)$$

For continuous case, such as Extended Kalman Filter (EKF) and Luenberger observer:

$$\begin{aligned} si_1(\tilde{x}_2, \tilde{x}_3) &= l_{11}\tilde{x}_2 + l_{12}\tilde{x}_3 \\ si_2(\tilde{x}_2, \tilde{x}_3) &= l_{21}\tilde{x}_2 + l_{22}\tilde{x}_3 \\ si_3(\tilde{x}_2, \tilde{x}_3) &= l_{31}\tilde{x}_2 + l_{32}\tilde{x}_3 \\ si_4(\tilde{x}_2, \tilde{x}_3) &= l_{41}\tilde{x}_2 + l_{42}\tilde{x}_3 \\ si_5(\tilde{x}_2, \tilde{x}_3) &= l_{51}\tilde{x}_2 + l_{52}\tilde{x}_3, \end{aligned} \quad (5)$$

where L is the matrix form of the observer gains l_{11}, \dots, l_{52} . For discontinuous case, such as sliding mode observer (SMO):

$$\begin{aligned} si_1(\tilde{x}_2, \tilde{x}_3) &= h_{11}S(\tilde{x}_2) + h_{12}S(\tilde{x}_3) \\ si_2(\tilde{x}_2, \tilde{x}_3) &= h_{21}S(\tilde{x}_2) + h_{22}S(\tilde{x}_3) \\ si_3(\tilde{x}_2, \tilde{x}_3) &= h_{31}S(\tilde{x}_2) + h_{32}S(\tilde{x}_3) \\ si_4(\tilde{x}_2, \tilde{x}_3) &= h_{41}S(\tilde{x}_2) + h_{42}S(\tilde{x}_3) \\ si_5(\tilde{x}_2, \tilde{x}_3) &= h_{51}S(\tilde{x}_2) + h_{52}S(\tilde{x}_3). \end{aligned} \quad (6)$$

Switching, however, induces chattering and thus continuous approximations are often adopted instead: $S(\tilde{x}_2) \approx l_{2eff}\tilde{x}_2$ and $S(\tilde{x}_3) \approx l_{3eff}\tilde{x}_3$. L can still be defined with effective gains l_{2eff} and l_{3eff} .

Define estimation errors as $\tilde{x} = x - \hat{x}$. Using prior information of the original system states, one can construct a projection mapping to ensure the boundedness of state estimates:

$$\begin{aligned} \hat{x}_i &= Proj_{\hat{x}_i}(\tau_i) \\ \tau_i &= \hat{f}_i + si_i \\ \hat{f}_i &= f_i(\hat{x}, \hat{a}_2). \end{aligned} \quad (7)$$

The projection mapping of a scalar is defined in [16] as

$$Proj_{\hat{x}_i}(\bullet_i) = \begin{cases} 0 & \text{if } \hat{x}_i = x_{imax} \text{ and } \bullet_i > 0 \\ 0 & \text{if } \hat{x}_i = x_{imin} \text{ and } \bullet_i < 0 \\ \bullet_i & \text{otherwise} \end{cases} \quad (8)$$

When applied to a vector \hat{x} , the project mapping is component-wise, i.e., $Proj_{\hat{x}}(\bullet) = [Proj_{\hat{x}_1}(\bullet_1), \dots, Proj_{\hat{x}_5}(\bullet_5)]^T$. It can be shown that for any adaptation function τ , the projection mapping used in (8) guarantees

(P1)

$$\hat{x} \in \Omega_x \triangleq \{\hat{x} : x_{imin} \leq \hat{x} \leq x_{imax}\}. \quad (9)$$

A slowly varying load torque can be treated by augmenting the state x with a_2 which will be adapted in the observer design. In addition, other slowly changing quantities, $R_r, a_5, a_7, a_8, a_{10}$, can also be treated as unknown parameters θ and extended for adaptation within the same design framework.

3.2 Observer Design

As a case study, the EKF is designed to simplify the gain tuning process as the Kalman gains are automatically adjusted along the state trajectory. With sampling rate of the filter as T_s and forward difference method, the system dynamics (2) can be discretized as

$$x_k = T_s f(x_{k-1}, u_{k-1}) + x_{k-1} = f'(x_{k-1}, u_{k-1}) \quad (10)$$

Linearization of the dynamics,

$$A = \frac{\partial f}{\partial x} = \begin{bmatrix} -a_3 & -a_1x_5 & a_1x_4 & a_1x_3 & -a_1x_2 \\ a_6x_5 & -a_7 & 0 & a_5 & a_6x_1 \\ -a_6x_4 & 0 & -a_7 & -a_6x_1 & a_5 \\ -a_9x_5 & a_{10} & 0 & -a_8 & -a_9x_1 \\ a_9x_4 & 0 & a_{10} & a_9x_1 & -a_8 \end{bmatrix} \quad (11)$$

Thus

$$A_k = T_s A + I \quad (12)$$

Predict:

Predicted state estimate

$$\hat{x}_{k|k-1} = f'(\hat{x}_{k-1|k-1}, u_{k|k-1}) \quad (13)$$

Predicted covariance estimate

$$P_{k|k-1} = A_{k-1}P_{k-1|k-1}A_{k-1}^T + Q_{k-1} \quad (14)$$

Update:

Measurement residual

$$\tilde{y}_k = z_k - C\hat{x}_{k|k-1} \quad (15)$$

Residual covariance

$$S_k = C_k P_{k|k-1} C_k^T + R_k \quad (16)$$

Near-optimal Kalman gain

$$K_k = P_{k|k-1} C_k^T S_k^{-1} \quad (17)$$

Updated state estimate

$$\hat{x}_{k|k} = \hat{x}_{k|k-1} + K_k \tilde{y}_k \quad (18)$$

Updated covariance estimate

$$P_{k|k} = (I - K_k C_k) P_{k|k-1}. \quad (19)$$

For general observer form

$$L = \frac{K_k}{T_s}. \quad (20)$$

4 Main Results: Integrated Control Design

We consider the control design for the simplified case where a system suffers from uncertainties \tilde{d} . For the induction motor case, uncertain nonlinearities could be result from the state estimation errors. The following practical assumption thus is required to establish stability results.

Assumption 4.1 *Uncertain nonlinearities are bounded, i.e.,*

$$\tilde{d} \in \Omega_{\tilde{d}} \triangleq \left\{ \tilde{d} : \|\tilde{d}\| \leq \delta_d \right\}, \quad (21)$$

where $\tilde{d} = d - d_n$, and δ_d is also a known bounding function.

With (P1) in (9), the state observer can guarantee the bounded state estimation error. The following assumption can be made for the control design,

Assumption 4.2 *The bounds of state estimation errors are known, i.e.,*

$$\tilde{x} \in \Omega_{\tilde{x}} \triangleq \{ \tilde{x} : \tilde{x}_{min} \leq \tilde{x} \leq \tilde{x}_{max} \} \quad (22)$$

where $\tilde{x}_{min} = [\tilde{x}_{1min}, \dots, \tilde{x}_{5min}]^T$ and $\tilde{x}_{max} = [\tilde{x}_{1max}, \dots, \tilde{x}_{5max}]^T$ are known.

The control design consists of four steps. Step 1 is the speed control loop with electromagnetic torque as an virtual control; step 2 is a robust torque control loop which regulates the electromagnetic torque from the speed loop in the first step; step 3 is the flux tracking loop which regulates the magnetic flux magnitude for efficient operation; step 4 delivers the required virtual control from step 3 using a similar robust control design. State estimation errors are explicitly taken into account within all control design steps as bounded model uncertainties. The controller and observer structure are illustrated in Fig. 1 with notations to be introduced in the following design steps.

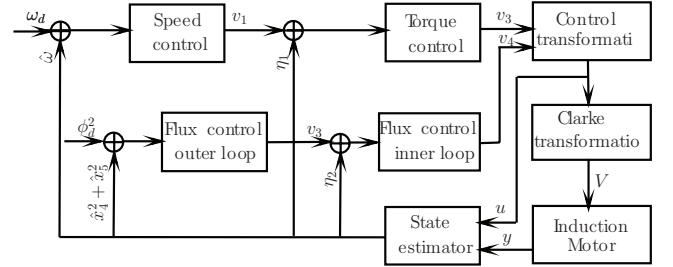


Fig. 1: Controller and observer structure.

4.1 Step 1–Speed Loop Control Design

Define the speed tracking error $z_1 = \hat{x}_1 - \omega_d$, and compute its time derivative

$$\dot{z}_1 = -a_3 z_1 + a_1(x_3 \hat{x}_4 - x_2 \hat{x}_5) + s i_1(\tilde{x}_2, \tilde{x}_3) - \dot{\omega}_d - a_3 \omega_d - \hat{a}_2. \quad (23)$$

Introduce a virtue control v_1 , and define the discrepancy between v_1 and the estimated electromagnetic torque $a_1(x_3 \hat{x}_4 - x_2 \hat{x}_5)$ as follows

$$z_2 = a_1(x_3 \hat{x}_4 - x_2 \hat{x}_5) - v_1. \quad (24)$$

Thus the speed tracking error can be rewritten as

$$\dot{z}_1 = -a_3 z_1 + v_1 + z_2 + s i_1(\tilde{x}_2, \tilde{x}_3) - \dot{\omega}_d - a_3 \omega_d - \hat{a}_2. \quad (25)$$

The virtual control v_1 is split into two parts

$$v_1 = v_{1a} + v_{1s}, \quad (26)$$

where v_{1a} is the feedforward model compensation given by

$$v_{1a} = -s i_1(\tilde{x}_2, \tilde{x}_3) + \dot{\omega}_d + a_3 \omega_d + \hat{a}_2, \quad (27)$$

and v_{1s} is the feedback stabilization control

$$v_{1s} = -k_{1s1} z_1. \quad (28)$$

Thus (25) can be rewritten as follows

$$\dot{z}_1 = -k_1 z_1 + z_2, \quad k_1 = a_3 + k_{1s1}. \quad (29)$$

Overall the virtual control v_1 is given by

$$v_1 = -k_{1s1}z_1 - s_{i1}(\tilde{x}_2, \tilde{x}_3) + \dot{\omega}_d + a_3\omega_d + \hat{a}_2, \quad (30)$$

and its derivative is computed as follows

$$\begin{aligned} \dot{v}_1 = & k_{1s1}k_1z_1 + \ddot{\omega}_d + a_3\omega_d + \hat{a}_2 \\ & + (l_{11}a_7 + l_{11}l_{21} + l_{12}l_{31})\tilde{x}_2 \\ & + (l_{12}a_7 + l_{11}l_{22} + l_{12}l_{32})\tilde{x}_3 \\ & - (l_{11}a_5 - l_{12}a_6\hat{x}_1)\tilde{x}_4 - (l_{12}a_5 + l_{11}a_6\hat{x}_1)\tilde{x}_5 \\ & - (l_{11}a_6x_5 - l_{12}a_6x_4)\tilde{x}_1 - k_{1s1}z_2, \end{aligned} \quad (31)$$

which will be used in the second step.

4.2 Step 2–Robust Torque Control Design

According to (24), (31), and (4), we have

$$\dot{z}_2 = v_2 + \psi_2 + \tilde{d}_2, \quad (32)$$

where $v_2 = a_{21}bu_1 + a_{22}bu_2$ with $a_{21} = -a_1\hat{x}_5$, $a_{22} = a_1\hat{x}_4$, and

$$\begin{aligned} \psi_2 = & -(a_7 + a_8)v_1 - a_1a_6\hat{x}_1(\hat{x}_4^2 + \hat{x}_5^2) \\ & - a_1a_9\hat{x}_1(\hat{x}_5x_3 + \hat{x}_4x_2) \\ & + a_1a_{10}(\hat{x}_2x_3 - \hat{x}_3x_2) + a_1x_3s_{i4}(\tilde{x}_2, \tilde{x}_3) \\ & - a_1x_2s_{i5}(\tilde{x}_2, \tilde{x}_3) - k_{1s1}k_1z_1 - \ddot{\omega}_d - a_3\dot{\omega}_d \\ & - \dot{\hat{a}}_2 - (l_{11}a_7 + l_{11}l_{21} + l_{12}l_{31})\tilde{x}_2 \\ & - (l_{12}a_7 + l_{11}l_{22} + l_{12}l_{32})\tilde{x}_3 + k_{1s1}z_2 \\ \tilde{d}_2 = & a_1a_5(\tilde{x}_5\hat{x}_4 - \tilde{x}_4\hat{x}_5) - a_1a_6x_1(\tilde{x}_4\hat{x}_4 + \tilde{x}_5\hat{x}_5) \\ & - a_1a_6\tilde{x}_1(\hat{x}_4^2 + \hat{x}_5^2) + (l_{11}a_5 - l_{12}a_6\hat{x}_1)\tilde{x}_4 \\ & + (l_{12}a_5 + l_{11}a_6\hat{x}_1)\tilde{x}_5 \\ & + (l_{11}a_6x_5 - l_{12}a_6x_4)\tilde{x}_1, \end{aligned} \quad (33)$$

where \tilde{d}_2 denotes the disturbance due to state estimation errors. One can try to estimate it which may result in improved system performance or reject it using the prior knowledge of its bounds. We here treat it as a bounded disturbance. The control v_2 is rewritten as follows

$$v_2 = v_{2a} + v_{2s}, \quad (34)$$

where the feedforward model compensation term is

$$v_{2a} = -\psi_2 - \tilde{d}_2 - z_1, \quad (35)$$

and the feedback stabilization term v_{2s} consists of the nominal stabilization term v_{2s1} and the robust control term v_{2s2}

$$\begin{aligned} v_{2s} = & v_{2s1} + v_{2s2}, \\ v_{2s1} = & -k_{2s1}z_2, \\ k_2 = & a_7 + a_8 + k_{2s1}. \end{aligned} \quad (36)$$

Thus (32) can be rearranged as follows

$$\dot{z}_2 = -k_2z_2 + v_{2s2} + \tilde{d}_2 - z_1. \quad (37)$$

Given Assumption 4.2, \tilde{d}_2 is bounded. Thus there exists v_{2s2} such that the following conditions hold

- $z_2(v_{2s2} + \tilde{d}_2) \leq \epsilon_2$,
- $z_2v_{2s2} \leq 0$,

where ϵ_2 is a design parameter and can be arbitrarily small. One example of v_{2s2} that satisfies above conditions can be taken as follows

$$v_{2s2} = -\frac{1}{4\epsilon_2}h_2^2z_2, \quad (38)$$

where $h_2 = \delta_{d_2}$ and δ_{d_2} is the bound of \tilde{d}_2 .

Remark 4.3 The aforementioned control v_1 and v_2 ensures that all signals are bounded. We define a positive definite function

$$V_{s2} = \frac{1}{2}z_1^2 + \frac{1}{2}z_2^2 \quad (39)$$

and have its time derivative

$$\begin{aligned} \dot{V}_{s2} = & -k_1z_1^2 + z_1z_2 + z_2\dot{z}_2 \\ = & -k_1z_1^2 - k_2z_2^2 + z_2(v_{2s2} + \tilde{d}_2) \\ \leq & -k_1z_1^2 - k_2z_2^2 + \epsilon_2 \\ \leq & -\lambda_2V_{s2} + \epsilon_2. \end{aligned} \quad (40)$$

Hence, V_{s2} is bounded above by

$$V_{s2} \leq \exp(-\lambda_2t)V_{s2}(0) + \frac{\epsilon_2}{\lambda_2}[1 - \exp(-\lambda_2t)], \quad (41)$$

where $\lambda_2 = 2 \min(k_1, k_2)$.

4.3 Step 3–Flux Outer Loop Control Design

Flux tracking control is designed using backstepping. Define the flux modules tracking error

$$z_3 = \hat{x}_4^2 + \hat{x}_5^2 - \psi_d, \quad (42)$$

and compute its time derivative

$$\dot{z}_3 = 2a_{10}(x_2\hat{x}_4 + x_3\hat{x}_5) + \psi_3, \quad (43)$$

where

$$\begin{aligned} \psi_3 = & -2a_8(\hat{x}_4^2 + \hat{x}_5^2) - 2a_{10}(\tilde{x}_2\hat{x}_4 + \tilde{x}_3\hat{x}_5) \\ & + 2l_{41}\tilde{x}_2\hat{x}_4 + 2l_{42}\tilde{x}_3\hat{x}_4 + 2l_{51}\tilde{x}_2\hat{x}_5 + 2l_{52}\tilde{x}_3\hat{x}_5 - \dot{\psi}_d. \end{aligned}$$

Note that ψ_3 depends on accessible signals. Introduce a virtual control v_3 , and a state z_4 to denote the discrepancy between v_3 and $2a_{10}(x_2\hat{x}_4 + x_3\hat{x}_5)$, i.e.,

$$z_4 = 2a_{10}(x_2\hat{x}_4 + x_3\hat{x}_5) - v_3. \quad (44)$$

Similar to v_1 , the virtual control v_3 is rewritten as

$$v_3 = v_{3a} + v_{3s}, \quad (45)$$

where the feedforward model compensation is $v_{3a} = -\psi_3$ and the feedback stabilization term $v_{3s} = -k_{3s1}z_3$. Thus we have

$$\dot{z}_3 = -k_3z_3 + z_4, \quad k_3 = k_{3s1}. \quad (46)$$

4.4 Step 4–Flux Inner Loop Control Design

The derivative of the virtue control discrepancy is

$$\dot{z}_4 = v_4 + \psi_4 + \tilde{d}_4, \quad (47)$$

where

$$\begin{aligned}
\psi_4 &= 2a_{10}a_5 (\hat{x}_4^2 + \hat{x}_5^2) - 2a_{10}a_7 (\hat{x}_2\hat{x}_4 + \hat{x}_3\hat{x}_5) \\
&+ 2a_{10} (l_{21}\tilde{x}_2\hat{x}_4 + l_{22}\tilde{x}_3\hat{x}_4 + l_{31}\tilde{x}_2\hat{x}_5 + l_{32}\tilde{x}_3\hat{x}_5) \\
&+ 2 (l_{41}\hat{x}_4 + l_{51}\hat{x}_5) (- (a_7 + l_{21}) \tilde{x}_2 - l_{22}\tilde{x}_3) \\
&+ 2 (l_{42}\hat{x}_4 + l_{52}\hat{x}_5) (-l_{31}\tilde{x}_2 - (a_7 + l_{32}) \tilde{x}_3) \\
&+ 2 (l_{41}\tilde{x}_2 + l_{42}\tilde{x}_3 + a_{10}\hat{x}_2 - 2a_8\hat{x}_4) \\
&\times (-a_8\hat{x}_4 - a_9\hat{x}_1\hat{x}_5 + a_{10}\hat{x}_2) \\
&+ 2 (l_{41}\tilde{x}_2 + l_{42}\tilde{x}_3 + a_{10}\hat{x}_2 - 2a_8\hat{x}_4) (l_{41}\tilde{x}_2 + l_{42}\tilde{x}_3) \\
&+ 2 (l_{51}\tilde{x}_2 + l_{52}\tilde{x}_3 + a_{10}\hat{x}_3 - 2a_8\hat{x}_5) \\
&\times (-a_8\hat{x}_5 + a_9\hat{x}_1\hat{x}_4 + a_{10}\hat{x}_3) \\
&+ 2 (l_{51}\tilde{x}_2 + l_{52}\tilde{x}_3 + a_{10}\hat{x}_3 - 2a_8\hat{x}_5) (l_{51}\tilde{x}_2 + l_{52}\tilde{x}_3) \\
&+ k_3 (-k_3 z_3 + z_4) - \ddot{\psi}_d \\
\tilde{d}_4 &= (2a_5 l_{41} \hat{x}_4 - 2a_6 l_{42} \hat{x}_4 \hat{x}_1 + 2a_5 l_{51} \hat{x}_5 - 2a_6 l_{52} \hat{x}_5 \hat{x}_1) \tilde{x}_4 \\
&+ (2l_{41} a_6 \hat{x}_1 \hat{x}_4 + 2l_{51} a_6 \hat{x}_1 \hat{x}_5 + 2l_{42} a_5 \hat{x}_4 + 2l_{52} a_5 \hat{x}_5) \tilde{x}_5 \\
&+ 2 (l_{41} \hat{x}_4 + l_{51} \hat{x}_5) a_6 \tilde{x}_1 x_5 - 2 (l_{42} \hat{x}_4 + l_{52} \hat{x}_5) a_6 \tilde{x}_1 x_4.
\end{aligned}$$

Note \tilde{d}_4 is the disturbance due to state estimation errors, and

$$\begin{aligned}
v_4 &= a_{21} b u_1 + a_{22} b u_2, \\
a_{41} &= 2a_{10} \hat{x}_4, \\
a_{42} &= 2a_{10} \hat{x}_5.
\end{aligned} \tag{48}$$

Design control input as

$$v_4 = v_{4a} + v_{4s}, \tag{49}$$

where the feedforward model compensation is

$$v_{4a} = -\psi_4 - z_3, \tag{50}$$

and the feedback stabilization control term consists of the nominal stabilization term v_{4s1} and the robust control term v_{4s2} ,

$$\begin{aligned}
v_{4s} &= v_{4s1} + v_{4s2}, \\
v_{4s1} &= -k_4 z_4.
\end{aligned} \tag{51}$$

Thus

$$\dot{z}_4 = -k_4 z_4 + v_{4s2} + \tilde{d}_4 - z_3. \tag{52}$$

From the assumption of the boundedness of state estimation error, there exists a v_{4s2} such that

- $z_4(v_{4s2} + \tilde{d}_4) \leq \epsilon_4$,
- $z_4 v_{4s2} \leq 0$,

where ϵ_4 is a design parameter which can be arbitrarily small. One example of v_{4s2} that satisfying above conditions is:

$$v_{4s2} = -\frac{1}{4\epsilon_4} h_4^2 z_4, \tag{53}$$

where $h_4 = \delta_{d_4}$ and δ_{d_4} is the bound of \tilde{d}_4 .

Remark 4.4 The control input can be determined by

$$\begin{bmatrix} u_1 \\ u_2 \end{bmatrix} = \frac{1}{b} \begin{bmatrix} -a_1 \hat{x}_5 & a_1 \hat{x}_4 \\ 2a_{10} \hat{x}_4 & 2a_{10} \hat{x}_5 \end{bmatrix}^{-1} \begin{bmatrix} v_{2a} + v_{2s} \\ v_{4a} + v_{4s} \end{bmatrix}. \tag{54}$$

For control input voltage to has unique solution, we have

$$\begin{vmatrix} -a_1 \hat{x}_5 & a_1 \hat{x}_4 \\ 2a_{10} \hat{x}_4 & 2a_{10} \hat{x}_5 \end{vmatrix} = -2a_1 a_{10} (\hat{x}_4^2 + \hat{x}_5^2) \neq 0, \tag{55}$$

which means flux modulus estimate should not be zero.

4.5 Stability Analysis

Remark 4.5 Control v_3 and v_4 guarantees the boundedness of z_3 and z_4 . Similar to the Remark 4.3, taking a Lyapunov function candidate

$$V_{s4} = \frac{1}{2} z_3^2 + \frac{1}{2} z_4^2 \tag{56}$$

and computing its time derivative, one can derive

$$V_{s4} \leq \exp(-\lambda_4 t) V_{s4}(0) + \frac{\epsilon_4}{\lambda_4} [1 - \exp(-\lambda_4 t)], \tag{57}$$

with $\lambda_4 = 2 \min(k_3, k_4)$. This implies the boundedness of z_3 and z_4 . If further assuming z_3 and z_4 dynamics are only subject to parametric uncertainties (i.e., $\tilde{d}_4 = 0$), the zero solution of z_3 and z_4 dynamics is asymptotically stable, i.e., $z_3, z_4 \rightarrow 0$, as $t \rightarrow \infty$.

To analyze the stability of the entire closed-loop system, we first define a Lyapunov function candidate

$$V_s = V_{s2} + V_{s4}. \tag{58}$$

Theorem 4.6 Given Assumption 4.2, the closed-loop system (2) with a state estimator (4) and the control u (54) has bounded states, and the Lyapunov function candidate V_s in (58) is bounded by

$$V_s \leq \exp(-\lambda t) V_s(0) + \frac{\epsilon}{\lambda} [1 - \exp(-\lambda t)], \tag{59}$$

with $\lambda = 2 \min(k_1, k_2, k_3, k_4)$.

Proof: Given the Lyapunov function candidate V_s and Assumption 4.2, we have

$$\begin{aligned}
\dot{V}_s &= -k_1 z_1^2 - k_2 z_2^2 - k_3 z_3^2 - k_4 z_4^2 \\
&+ z_2 (v_{2s2} + \tilde{d}_2) + z_4 (v_{4s2} + \tilde{d}_4) \\
&\leq -k_1 z_1^2 - k_2 z_2^2 - k_3 z_3^2 - k_4 z_4^2 + \epsilon_2 + \epsilon_4 \\
&\leq -\lambda V_s + \epsilon,
\end{aligned} \tag{60}$$

which implies (59) and the boundedness of all states. This completes the proof.

5 Simulation Results

In this section, we present simulation results for the proposed speed sensorless control algorithm which includes the EKF as an state observer. The goal is to demonstrate the following:

- 1) the proposed method can achieve high bandwidth (200Hz) and high precision speed sensorless tracking control of a typical induction motor under practical implementation constraints (20KHz sampling rate and 400V input saturation) with only stator voltage and current measurements;
- 2) the gain selection for the proposed method is straightforward;
- 3) the proposed method can track various trajectories as long as the state and control input constraints are considered. No dependence of controller and/or observer on the trajectory is found.

The simulation is implemented in Matlab with sampling rate of 20KHz and the following induction motor parameters [2] $R_s = 2.3\Omega$, $R_r = 4.95\Omega$, $L_m = 0.523H$, $L_s =$

0.538H, $L_r = 0.5396H$, $J = 0.02kg.m^2$, $b_1 = 0.001$, $np = 2$, and $T_f = 0.50$.

To achieve the control bandwidth of 200Hz, the control gains are selected as $k_1 = k_2 = k_3 = k_4 = 1200$, and no further gain tuning is necessary. As a result, there is no fundamental limitation on the achievable control bandwidth, as long as the control input is not severely saturated before the observer, which is independent from the controller, converges. The desired flux modulus is $\phi_d = 0.5$ for all cases.

The initial condition for the states are $x = [\omega_d(0), 2, 2, 0.5, 0.5]^T$, where $\omega_d(0)$ is the desired speed at $t = 0$. The control inputs has a saturation limit of 400V. The observer has initial estimation errors of 10 percent. For implementation of EKF, the current measurements are assumed to have noises of 2mA and the process noises are all assumed to be $0.001 \times T_s$.

We tested the proposed observer-controller by tracking different trajectories. Fig. 2 shows the high-bandwidth tracking of 200Hz sinusoidal trajectory. After the short transient for the observer to converge, the controller tracks the speed reference signal closely. Fig. 3 shows the simulations result of tracking a step reference speed signal, which is first filtered by a second order critically damped transfer function with 200Hz natural frequency. The tracking transient shows small settling time close to 1/200 second. Fig. 4 further demonstrates the excellent tracking performance for a ramp up and down speed reference trajectory. The controller performs consistently well for all tested trajectories, and the closed-loop system performance appears to be independent of the reference trajectory.

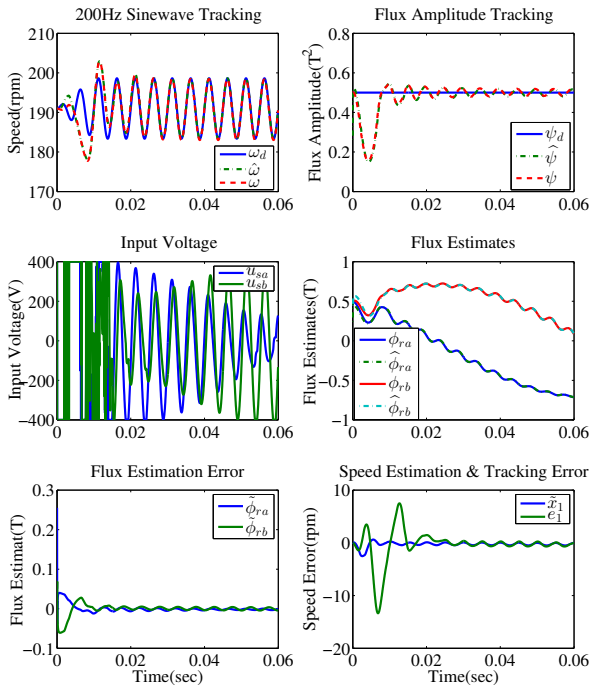


Fig. 2: Tracking of 200Hz sinusoidal trajectory.

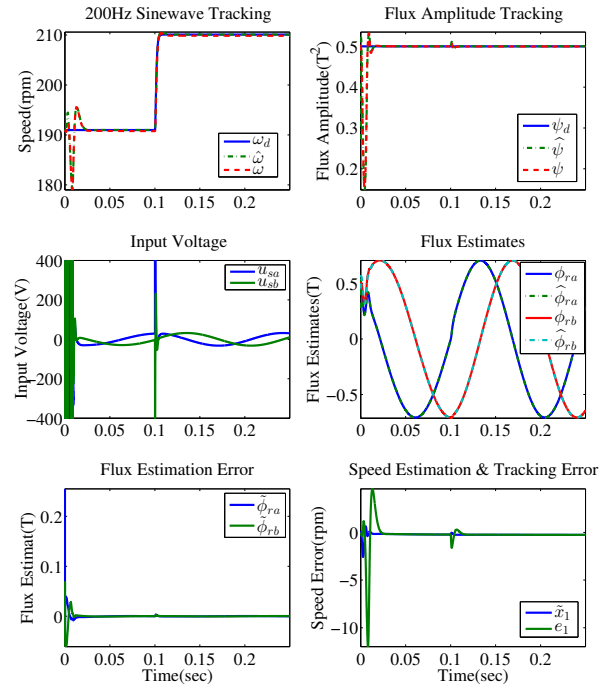


Fig. 3: Tracking a step reference with 0.005sec(200Hz) settling time.

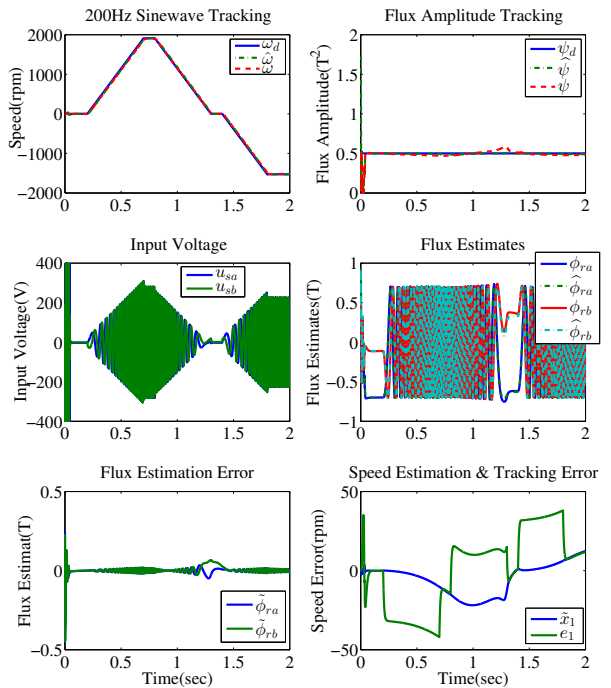


Fig. 4: Tracking a ramp reference trajectory.

6 Conclusion and Future Work

In this paper, we proposed an integrated control and observer design framework for speed sensorless control of induction motors with only current measurements. With a general observer structure, the backstepping-based robust control design explicitly considers all the state estimation and tracking errors. Simulation results shown that the proposed method leads to high bandwidth and high precision speed sensorless tracking control of a typical induction motor under practical implementation constraints, in contrast to the severe bandwidth and performance limitations inherent to previous methods. Ongoing work includes experimental verification of the proposed method.

References

- [1] M. Montanari, S. M. Peresada, C. Rossi, and A. Tilli, "Speed sensorless control of induction motors based on a reduced-order adaptive observer," vol. 15, no. 6, pp. 1049–1064, 2007.
- [2] H. K. Khalil, E. G. Strangas, and S. Jurkovic, "Speed observer and reduced nonlinear model for sensorless control of induction motors," *Control Systems Technology, IEEE Transactions on*, vol. 17, no. 2, pp. 327–339, 2009.
- [3] R. Marino, P. Tomei, and C. M. Verrelli, *Induction Motor Control Design*. London, UK: Springer, 2010.
- [4] J. Chiasson, "Dynamic feedback linearization of the induction motor," vol. 38, no. 10, pp. 1588–1594, 1993.
- [5] L. Harnefors, "Globally stable speed-adaptive observers for sensorless induction motor drives," vol. 54, no. 2, pp. 1243–1245, Apr. 2007.
- [6] D. J. Atkinson, P. P. Acarnley, and J. W. Finch, "Observers for induction motor state and parameter estimation," vol. 27, no. 6, pp. 1119–1127, Nov./Dec. 1991.
- [7] C. Schauder, "Adaptive speed identification for vector control of induction motors without rotational transducers," vol. 28, no. 5, pp. 1054–1061, Sep./Oct. 1992.
- [8] H. Kubota, K. Matsuse, and T. Nakano, "DSP-based speed adaptive flux observer of induction motor," vol. 29, no. 2, pp. 344–348, Mar./Apr. 1993.
- [9] H. Kubota and K. Matsuse, "Speed sensorless field-oriented control of induction motor with rotor resistance adaption," vol. 30, no. 5, pp. 1219–1224, Sep./Oct. 1994.
- [10] K. Ohya, G. M. Asher, and M. Sumner, "Comparative analysis of experimental performance and stability of sensorless induction motor drives," vol. 53, no. 1, pp. 178–186, Feb. 2006.
- [11] C. Lascu, I. Boldea, and F. Blaabjerg, "A class of speed-sensorless sliding-mode observers for high-performance induction motor drives," vol. 56, no. 9, pp. 3394–3403, Sep. 2009.
- [12] M. Ghanes and G. Zheng, "On sensorless induction motor drives: sliding-mode observer and output feedback controller," vol. 56, no. 9, pp. 3404–3413, Sep. 2009.
- [13] S. Solvar, B. Le, M. Ghanes, J. P. Barbot, and G. Santomenna, "Sensorless second order sliding mode observer for induction motor," in *IEEE International Conference on Control Applications*, Yokohama, Japan, 2010, pp. 1933–1938.
- [14] M. Hilaiet, F. Auger, and E. Berthelot, "Speed and rotor flux estimation of induction machines using a two-stage extended kalman filter," vol. 45, no. 8, pp. 1819–1827, Aug. 2009.
- [15] W. Leonhard, *Control of Electrical Drives*. Springer, 2001.
- [16] B. Yao and M. Tomizuka, "Adaptive robust control of siso nonlinear systems in a semi-strict feedback form," *Automatica*, vol. 33, no. 5, pp. 893–900, 1997.